ELSEVIER

Journal of Nuclear Materials 248 (1997) 180–184

journal of nuclear materials

Application of a mechanistic model for radiation-induced amorphization and crystallization of uranium silicide to recrystallization of UO_2

J. Rest *

Energy Technology Division, Argonne National Laboratory, 9700 South Cass Ave., Argonne, IL 60439-4837, USA

Abstract

An alternative mechanism for the evolution of recrystallization nuclei is described for a model of irradiation-induced recrystallization of UO_2 wherein the stored energy in the UO_2 is concentrated in a network of sinklike nuclei that heretofore were assumed to diminish with dose due to interaction with radiation-produced defects. The sinklike nuclei are identified as cellular dislocation structures that evolve relatively early in the irradiation period. In the alternative approach, a generalized theory of radiation-induced amorphization and crystallization, developed for uranium silicide, is applied to UO_2. The complicated kinetics involved in the formation of a cellular dislocation network are approximated by the formation and growth of subgrains due to the interaction of shock waves produced by fission-induced damage to the UO_2. © 1997 Elsevier Science B.V.

1. Introduction

The peripheral region of UO_2 fuel pellets reveals an increasingly porous microstructure with burnup [1–4]. Observations of this 'rim effect' show that an extremely fine-grained structure formed by recrystallization of the original grains is associated with this porous microstructure. TEM observations [5] of the formation mechanism of the recrystallized region show that dislocation density increases with burnup. Low-angle boundaries begin to form above $\sim 8 \times 10^{26}$ fissions/m^3 (30 GW d/t). Subdivided grains 20–30 nm in size and with high-angle boundaries due to the accumulation of an extremely high density of subboundaries, together with recrystallized grains 50–200 nm in size and adjacent to the subdivided grain region are observed in fuel irradiated to $\sim 2.2 \times 10^{27}$ fissions/m^3 (83 GW d/t).

This is essentially the physical picture that was proposed as the basis of a model for irradiation-induced recrystallization wherein the stored energy in the UO_2 is concentrated in a network of sinklike nuclei that diminish with dose due to interaction with radiation-produced defects [6]. The sinklike nuclei are identified as cellular dislocation structures that evolve relatively early in the irradiation period. Impurities formed during fissioning of the UO_2 diffuse as vacancy-impurity complexes to cell walls where they effectively pin the wall, i.e., dislocation movement to and from the wall is hindered. The walls containing no impurities continue to undergo subgrain coalescence that results in viable nuclei for recrystallization. Recrystallization is induced when the energy per nucleus is high enough that the creation of grain-boundary surfaces is offset by the creation of strain-free volumes, with a resultant net decrease in the free energy of the UO_2. This formulation was shown to provide a plausible interpretation of the fission density at which grain subdivision begins.

Nevertheless, the idea that vacancy-solute pairs formed during irradiation of UO_2 migrate to cell walls and pin the wall is based on indirect evidence [6,7], not on direct experimental evidence. The primary purpose of this paper is to show that an alternative mechanistic description of the evolution of recrystallization nuclei, consistent with observation, can be achieved by a utilization of a generalized theory of radiation-induced amorphization and crystallization developed for intermetallic nuclear materials.

* Tel.: +1-708 252 5026; fax: +1-708 252 4798; e-mail: rest@maat.mct.anl.gov.

PII S0022-3115(97)00117-7

2. Model

The model for radiation-induced recrystallization described in Ref. [6] is based, in part, on the following assumptions:

– A cellular dislocation structure evolves relatively early in the irradiation period.

– Impurities formed during fissioning of the material diffuse to cell walls as vacancy/impurity complexes. The impurities effectively pin the wall, i.e., dislocation movement to and from the wall is retarded.

– Not all cell walls are uniformly affected by impurities; the walls that contain no impurities continue to undergo subgrain coalescence, which results in viable recrystallization nuclei.

Based on the above discussion, a number, C_s, of recrystallization nuclei are assumed per unit volume of material. It appears that these nuclei form relatively early in the irradiation period at low values of stored energy and that they are associated with microstructural features such as subgrain-boundary triple points or walls of cellular dislocation structures. Recrystallization nuclei act as sinks for irradiation-produced defects. As the irradiation proceeds, the nuclei are eliminated by interaction with vacancy-solute pairs. In other words, the concentration of impurities reduces the mobility of the interface [7]. Many potential solute atoms are produced during fission, e.g., gas atoms and rare earths. Thus, the available stored energy is concentrated on fewer and fewer nuclei (one can consider that the nuclei are holes in the material and that they act as stress concentrators), with a resultant increase in average energy per nucleus. Recrystallization is induced when the energy per nucleus is high enough to offset the creation of a grain boundary surface by creating a strain-free volume, with a resultant net decrease in the free energy of the material.

The concentration of recrystallization nuclei, c_s, is given by [6]

$$\frac{1}{c_s}\frac{dc_s}{dt} = -\frac{28\pi r_{sm} c_I D_{vI} \omega_4^v c_v}{\Omega\left(c_i + 7\omega_3^v/12\,\omega_0^i\right)\omega_0^i}, \tag{1}$$

where c_v, c_i, and c_I are the vacancy, interstitial, and impurity concentrations, respectively; r_{sm} is the annihilation radius of a recrystallization nucleus/vacancy-solute pair; D_{vI} is the diffusivity of the vacancy-solute pair; and Ω is the atomic volume. ω_0^v and ω_4^v are the jump frequencies of vacancies and interstitials, respectively, unperturbed by the presence of a solute atom, ω_3^v and ω_4^v are the jump rates of vacancies away from and toward nearest-neighbor nuclei of solute atoms.

The concentration of viable recrystallization nuclei, which results from the integration of Eq. (1), is quite different from that given by classical nucleation theory in that the concentration decreases with fluence instead of increasing with irradiation until the nucleation barrier is surmounted and the higher energy state of the crystal forms. In the present case, the nuclei are formed early in the irradiation by the damage process at relatively low values of strain energy. As the irradiation proceeds and the nuclei are eliminated by interaction with the vacancy-solute pairs, the available stored energy is concentrated in fewer and fewer nuclei, thus increasing the energy per nucleus.

Recrystallization is induced when the energy per nucleus is high enough that the creation of grain-boundary surfaces is offset by the creation of strain-free volumes, with a resultant net decrease in the free energy of the material. The stored energy, E_s, is taken to be concentrated in the network, c_s, and the minimum standard free energy of formation of a nucleus, ΔG, is assumed to have a rate of change with respect to a change in c_s given by Boltzmann's law, i.e.,

$$\frac{d\Delta G}{dc_s} = -\frac{kT}{c_s}. \tag{2}$$

By equating c_s obtained from Eq. (1) to the value of c_s obtained from Eq. (2) where a relatively small energy fluctuation can allow the system to jump over the energy barrier and cause the creation of a relatively defect-free crystal of material, a relation for the value of the fission density, FDX (m^{-3}), at which recrystallization will occur is obtained, i.e.,

$$\mathrm{FDX} = \frac{E_{sf}\dot{f}\Omega\left(c_i + 7\omega_3^v/12\,\omega_0^i\right)\omega_0^i}{28\pi r_{sm} kTc_I D_{vI}\omega_4^v c_v}, \tag{3}$$

where $\dot{f}$ is the fission rate, and $E_{sf} = E_s + \Delta G$.

As discussed in the introduction, the idea that vacancy-solute pairs formed during irradiation of UO_2 migrate to cell walls and pin the wall is based on indirect rather than direct experimental evidence. Thus, it is of interest to ascertain other potential mechanisms for the evolution of the recrystallization nuclei (i.e., as compared to that expressed by Eq. (1)). A rate-theory model [8] for ion-induced crystallization and amorphization of U_3Si has been generalized to include U_3Si_2 [9]. The model is based on the fact that the bombardment of solids by energetic particles produces displacements of the host atoms and thus damage to the structure of the solids. If the damage energy is sufficiently high, displacement cascades containing hundreds of atoms each are produced. The early stages of cascade development are characterized by the formation of shock waves [10–15], and that in some materials (e.g., Si, U_3Si, U_3Si_2) amorphous material is left after the cascades cool to ambient temperature [16]. In other materials (such as UO_2), the 'molten' material within the damage cascade crystallizes upon 'cooling.' Within the context of the model, the bombarding ions produce clusters of amorphous material that are considered centers of expansion (CE), or excess free volume zones. Simultaneously,

centers of compression (CC) are created in the material. The CCs are local regions of increased density that travel through the material as an elastic (e.g., acoustic) shock wave. The CEs can be annihilated upon contact with a sufficient number of CCs, forming either a crystallized region that is indistinguishable from the host material, or a region with a slight disorientation (crystallized grain). The CCs can also annihilate each other upon contact, forming either oriented or slightly disoriented crystal structures. Crystallized grains grow by accumulating additional CCs. Full amorphization (or full crystallization) is calculated on the basis of achieving a volume fraction consistent with the close packing of spherical entities.

The full set of equations describing the behavior of the CEs and the CCs is given in Ref. [9]. The time rate of change of the density (in units of atom fraction) of crystallized grains, C_g, is given by

$$\frac{dC_g}{dt} = \beta_1 f_1 \frac{N_{ce}}{N_{cc}} v_a C_{cc} C_{ce} - \beta_3 f_3 v_{cc} C_{cc} C_{cc} - N_{ce} K \xi_g V_\alpha C_g, \tag{4}$$

where β_1 and β_3 are the probabilities that the interaction between a CE and a CC, and between a CC and a CC, respectively, results in a crystallized grain (instead of a resultant atom orientation that is in alignment with the original grain structure), v_{cc} is the velocity of the shock wave in the material, K is the damage rate in displacements per atom per second (dpa/s), N_{ce} and N_{cc} are the atom fraction of CEs and CCs created per dpa, $V_\alpha = V_c N_0$, where V_c is the volume of amorphous material created per N_{ce}, and N_0 is the number of atoms per unit volume. The last term in Eq. (4) is the loss of crystallized grain nuclei due to amorphization by an incoming ion. ξ_g is the probability that for amorphous clusters which are unstable and recrystallize during the solidification of the cascade, the nuclei is left intact. The radius of the crystallized grains is given by

$$R_g = \left(\frac{V_g}{4\pi/3} \right)^{1/3}, \tag{5}$$

where

$$V_g = \frac{V_g^f}{C_g}, \tag{6}$$

and

$$\frac{dV_g^f}{dt} = \beta_2 f_2 v_x C_{cc} C_g R_g^2 A_{cc} - \delta R_g N_{ce} K \xi_g V_\alpha. \tag{7}$$

In Eq. (7), β_2 is the probability that an interaction between a CC and a crystallized grain results in the growth of the grain (as compared to formation of a region of the material adjacent to the crystallized grain whose atoms are in alignment with the crystal structure of the host atoms), $A_{cc} = 2\pi(\eta_{cc}\Omega/(4\pi/3))^{2/3}$ is the effective surface area of a CC, and η_{cc} is the fractional density decrease that occurs upon the creation of a CC. In Eq. (7), it is assumed that the interaction between a CC and a crystallized grain can be described by the Gibbs theory of surfaces. The first term of Eq. (7) describes the growth of crystallized grains by accumulation of CCs. The last term in Eq. (7) is the loss of crystallized grain volume due to amorphization by an incoming ion. It is assumed here that interaction between the CEs, the CCs, and crystallized grains is facilitated by irradiation produced defects. For example, CC annihilation upon contact, forming either oriented or slightly disoriented crystal structures, may be facilitated by the presence of radiation-produced defects. Thus the rate constants, f_1–f_3, include not only the standard interaction cross sections, but the probability of finding an appropriate number of irradiation produced defects in the near vicinity of the interaction site.

The generalized model [9] has been applied to ion-irradiation and in-reactor experiments on U_3Si and U_3Si_2 and provides an interpretation for the amorphization curve (dose required to amorphize the material as a function of temperature), for the ion-radiation-induced nanoscale polycrystallization of these materials at temperatures above the critical temperature for amorphization, as well as for the role of the small crystallites in retarding amorphization.

To apply this model to UO_2 the activation energies for crystallization of an amorphous cluster by a CC, and for irradiation-enhanced crystallization were decreased by the ratio of the melting temperature of U_3Si and UO_2, the activation energies for thermal crystallization and for grain growth due to interaction between a CC and a crystallized grain were increased by the ratio of the melting temperature, and the number of CEs created per dpa was reduced by the ratio of the UO_2 and U_3Si densities. In addition, it is assumed that for UO_2, the amorphous clusters formed in the damage cascades are very unstable and quickly crystallize. This is consistent with ion irradiation data that shows that UO_2 remains crystalline at 20 K [17].

Fig. 1 shows the calculated grain density, C_g, from Eq. (4), and grain diameter, $2R_g$, from Eqs. (5)–(7), as a function of fission density for an irradiation at 623 K and an average fission rate of 1×10^{19} fissions/m^{3}s. C_g peaks relatively early in the irradiation period. Unlike U_3Si and U_3Si_2, where crystallized grain nuclei are formed primarily by the annihilation of amorphous clusters by shock waves, recrystallization nuclei in UO_2 are formed by the interaction between shock waves. This process is also present in the intermetallics, but at a much lower level than that provided by CC–CE annihilation. Also shown in Fig. 1 is the concentration of viable recrystallization nuclei, C_s, which results from the integration of Eq. (1). Comparing C_s with C_g confirms the interpretation that these nuclei form relatively early in the irradiation period at low values of stored energy and that they are associated with microstructural features such as subgrain-boundary triple points or walls of cellular dislocation structures. It is clear from Fig. 1 that subsequent to the initial buildup of

crystallized grains, C_s follows the trend of the calculated density of crystallized grains, C_g, obtained from the theory of radiation-induced amorphization and crystallization. In addition, the calculated behavior of R_g as a function of burnup is consistent with the observations reported by Nogita and Une [5,18] that low-angle boundaries begin to form above $\sim 8 \times 10^{26}$ fissions/m^3 (indicated by a circled 1 in Fig. 1), and that subdivided grains 20–30 nm in size and recrystallized grains 50–200 nm in size adjacent to the subdivided grains exist in fuel irradiated to about 2.2×10^{27} fissions/m^3 (indicated by a circled 3 in Fig. 1). The theory of radiation-induced recrystallization (i.e., Eq. (3)) predicts that recrystallization is initiated at $\sim 1.5 \times 10^{27}$ fissions/m^3 (indicated by a circled 2 in Fig. 1).

A striking aspect of the observed bubble population subsequent to recrystallization is that they appear uniformly distributed and non-interacting [6]. It is assumed here that this bubble population inhabits fixed sites. These sites are formed upon grain recrystallization and are associated with nodes that are formed by the intersection of grain edges within the subgrain boundary structure. Upon intersection, fission gas that collects along grain edges vents to these nodes where it is trapped. Gas bubbles at

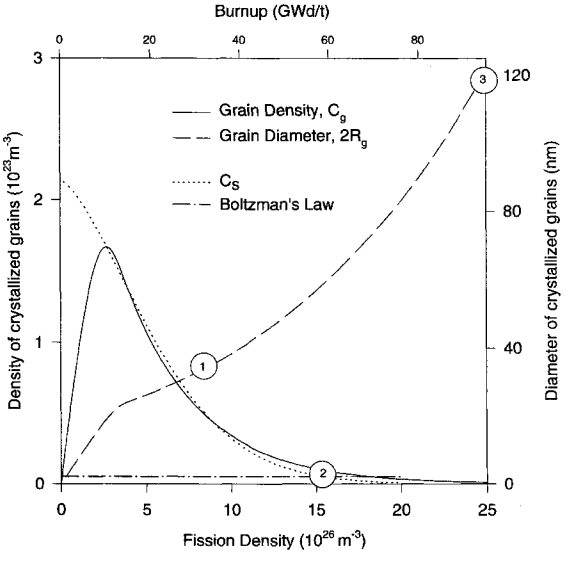

Fig. 1. Calculated grain density, C_g, and grain diameter, $2R_g$, based on theory of radiation-induced amorphization and crystallization as a function of fission density for irradiation at 623 K and average fission rate of 1×10^{19} fissions/m^{3}s. Also shown is the concentration of viable recrystallization nuclei, C_s, which results from integration of Eq. (1). Observations reported by Nogita and Une [5,18]: low-angle boundaries begin to form above $\sim 8 \times 10^{26}$ fissions/m^3 (indicated by a circled 1), and subdivided grains 20–30 nm in size and recrystallized grains 50–200 nm in size exist in fuel irradiated to $\sim 2.2 \times 10^{27}$ fissions/m^3 (indicated by a circled 3). Prediction of the theory of radiation-induced recrystallization (given by Eq. (3)), that recrystallization is initiated at $\sim 1.5 \times 10^{27}$ fissions/m^3, is indicated by a circled 2.

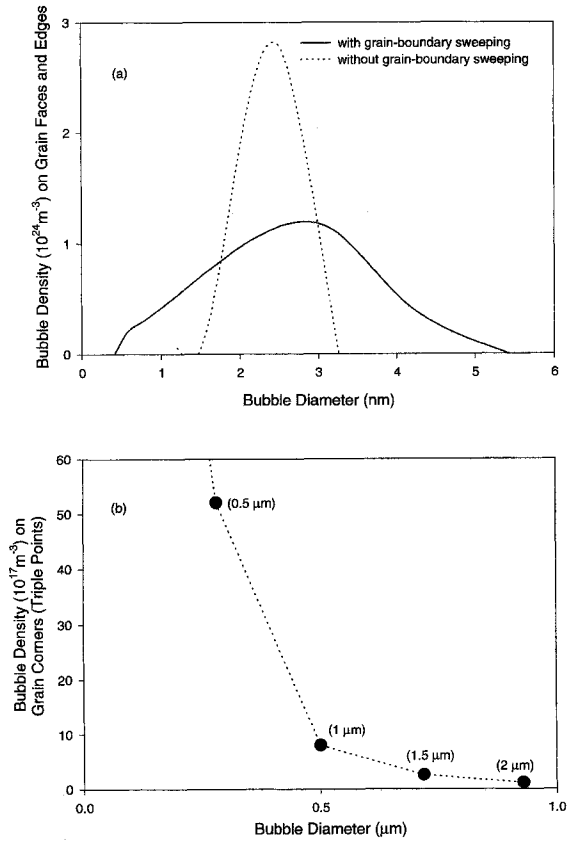

Fig. 2. (a) Fission-gas-bubble size distributions on grain faces and edges calculated with GRASS-SST [19] with and without the effects of subgrain growth/grain-boundary sweeping. The irradiation conditions and grain growth kinetics shown in Fig. 1 were utilized in the calculation. (b) Calculated bubble distribution on grain corners (triple points) made assuming that recrystallization, denoted by a circled 2 in Fig. 1, leads to the formation of grains with sizes given by the numbers in parentheses.

these 'dead-end' nodes grow as they continue to collect additional gas. If the grains are assumed to be cubes, and the 'dead-end' nodes are taken to be grain corners formed by the intersection of six grain edges, the number of nodes per cubic centimeter is given by the inverse of the cube root of the grain diameter, i.e., $C_N = d_g^{-1/3}$.

Fig. 2(a) shows intergranular fission-gas-bubble size distributions calculated with GRASS-SST [19] with and without the effects of subgrain growth/grain-boundary sweeping [20]. The irradiation conditions and grain growth kinetics shown in Fig. 1 were utilized in the calculation. For the case of no grain growth, a fixed grain size of 120 nm was used. The results shown in Fig. 2(a) demonstrate that subgrain growth and boundary sweeping result in a coarsened intergranular bubble distribution. In addition, the GRASS-SST calculations show that the intergranular bubbles have interconnected to form grain-boundary tun-

nels. The subsequent venting of these tunnels to fixed grain-corner sites enables the gas to accumulate and form 0.5–2 μm size bubbles, as shown in Fig. 2(b). The calculated bubble distribution on grain corners (triple points) shown in Fig. 2(b) was made assuming that recrystallization, denoted by a circled 2 in Fig. 1, leads to the formation of grains with sizes given by the numbers in parentheses (i.e., 0.5, 1, 1.5, and 2 μm). These results follow the trend of the observations [18].

3. Discussion

An estimate of the cell size of a cellular dislocation structure evolved from shock–wave interaction can be obtained from a consideration of the limited range of energies at which a damage event may be able to create a great enough density of fast recoils to form a shock wave [14]. For uranium ions in uranium metal, the maximum energy transfer is about 0.5 keV and occurs at an energy of about 4 keV. If one assumes that this energy transfer goes into creating dislocation loops having a radius equal to the Burgers vector, then in UO_2 a shock wave–shock wave (i.e., CC–CC) interaction will produce about 15 loops. Coalescence of these loops into a cubic cellular configuration results in a cell size of about 2 nm.

In the more 'stable' UO_2, amorphous clusters do not survive cascade 'cooling.' It is possible that a crystallized region is formed in the wake of cascade solidification, but this would lead to very high crystallization rates (in U_3Si, nanocrystals are formed above the critical temperature for amorphization at a rate of about one per ion), leading to saturation of the material with nanocrystals within several tenths of a dpa. In this case, in order to explain the evolution of the dislocation and subgrain structure reported in Ref. [18], a mechanism of nanocrystal destruction would have to be postulated as strong enough to delay the filling of space with crystallized material from several dpa to thousands of dpa. Observations of UO_2 irradiated at room temperature with 500 keV Xe ions to 10^{20} ions/m^2 are not consistent with this mechanism [17]. Instead, the observations show an increased dislocation density and the presence of small subgrains separated with the edges of the dislocations. Thus, within the context of the model presented in this paper, it seems plausible to postulate that the primary mechanism available to form recrystallized grain nuclei in UO_2 is shock wave–shock wave annihilation.

Acknowledgements

This work was supported by US Department of Energy, Office of Arms Control and Nonproliferation, under Contract W-31-109-Eng-38.

References

[1] N.E. Cunningham, M.D. Freshley, D.D. Lanning, J. Nucl. Mater. 188 (1992) 19.
[2] T. Kameyama, T. Matsumura, M. Kinoshita, Proc. ANS Topical Meeting on LWR Fuel Performance, Avignon, France, 1991, p. 620.
[3] K. Une, K. Nogita, S. Kashibe, M. Imamura, J. Nucl. Mater. 188 (1992) 65.
[4] L.E. Thomas, C.E. Beyer, L.A. Charlot, J. Nucl. Mater. 188 (1992) 80.
[5] K. Nogita, K. Une, Nucl. Instr. Meth. B91 (1994) 301.
[6] J. Rest, G.L. Hofman, J. Nucl. Mater. 210 (1994) 187.
[7] S.J. Zinkle, R.A. Dodd, G.L. Kulcinski, in: Proc. Effects of Radiation on Materials, 12th Int. Symp., ASTM-STP 870, eds. F.A. Garner and J.S. Perkin (American Society for Testing and Materials, Philadelphia, PA, 1985) p. 363.
[8] J. Rest, J. Nucl. Mater. 225 (1995) 308.
[9] J. Rest, J. Nucl. Mater. 240 (1997) 205.
[10] M. Guinan, J. Nucl. Mater. 53 (1974) 171.
[11] Y. Hayashiuchi, Y. Kitazoe, T. Sekiya, Y. Yamamura, J. Nucl. Mater. 71 (1977) 181.
[12] Y. Kitazoe, Y. Yamamura, Radiat. Eff. Lett. 50 (1980) 39.
[13] G. Carter, Radiat. Eff. Lett. 50 (1980) 105.
[14] K.W. Winterbon, Radiat. Eff. Lett. 57 (1980) 89.
[15] V.P. Zhukov, A.V. Ryabenko, Radiat. Eff. 82 (1984) 85.
[16] T. Diaz de la Rubia, G.H. Gilmer, UCRL-116382 (1994).
[17] Hj. Matzke, L.M. Wang, J. Nucl. Mater. 231 (1996) 155.
[18] K. Nogita, K. Une, J. Nucl. Mater. 226 (1995) 302.
[19] J. Rest, NUREG/CR-0202, ANL-78-53, Argonne National Laboratory (1978).
[20] J. Rest, A.W. Cronenberg, J. Nucl. Mater. 150 (1987) 203.